

# DISCOVERY OF THE OPTICAL COUNTERPART AND EARLY OPTICAL OBSERVATIONS OF GRB990712<sup>a</sup>

<sup>a</sup>BASED ON OBSERVATIONS COLLECTED AT SAAO, SUTHERLAND; ESO, PARANAL AND LA SILLA (ESO PROGRAMS 63.O-0618 AND 63.O-0567); AND AAT, AUSTRALIA.

K.C. SAHU<sup>2</sup>, P. VREESWIJK<sup>3</sup>, G. BAKOS<sup>2,4</sup>, J.W. MENZIES<sup>5</sup>, A. BRAGAGLIA<sup>6</sup>, F. FRONTERA<sup>7</sup>, L. PIRO<sup>8</sup>, M. D. ALBROW<sup>9</sup>, I. A. BOND<sup>10</sup>, R. BOWER<sup>11</sup>, J. A. R. CALDWELL<sup>5</sup>, A. J. CASTRO-TIRADO<sup>12,13</sup>, F. COURBIN<sup>14</sup>, M. DOMINIK<sup>15</sup>, J.U. FYNBO<sup>31</sup>, T. GALAMA<sup>3,16</sup>, K. GLAZEBROOK<sup>17</sup>, J. GREENHILL<sup>18</sup>, J. GOROSABEL<sup>12</sup>, J. HEARNSHAW<sup>9</sup>, K. HILL<sup>18</sup>, J. HJORTH<sup>19</sup>, S. KANE<sup>18</sup>, P. M. KILMARTIN<sup>9</sup>, C. KOUVELIOTOU<sup>20</sup>, R. MARTIN<sup>21</sup>, N. MASETTI<sup>7</sup>, P. MAXTED<sup>22</sup>, D. MINNITI<sup>14</sup>, P. MØLLER<sup>23</sup>, Y. MURAKI<sup>24</sup>, T. NAKAMURA<sup>25</sup>, S. NODA<sup>24</sup>, K. OHNISHI<sup>26</sup>, E. PALAZZI<sup>7</sup>, J. VAN PARADIJS<sup>3,27</sup>, E. PIAN<sup>7</sup>, K. R. POLLARD<sup>9</sup>, N.J. RATTENBURY<sup>10</sup>, M. REID<sup>28</sup>, E. ROL<sup>3</sup>, T. SAITO<sup>29</sup>, P. D. SACKETT<sup>15,17</sup>, P. SAIZAR<sup>30</sup>, C. TINNEY<sup>17</sup>, P. VERMAAK<sup>5</sup>, R. WATSON<sup>18</sup>, A. WILLIAMS<sup>21</sup>, P. YOCK<sup>10</sup>, A. DAR<sup>32</sup>

*Draft version April 26, 2024*

<sup>2</sup>Space Telescope Science Institute, 3700 San Martin Drive, Baltimore, MD 21218, USA

<sup>3</sup>Astronomical Institute “Anton Pannekoek”, University of Amsterdam, Kruislaan 403, 1098 SJ Amsterdam, The Netherlands

<sup>4</sup>Konkoly Observatory, PO Box 67, 1525 Budapest, Hungary

<sup>5</sup>South African Astronomical Observatory, P.O. Box 9, Observatory 7935, South Africa

<sup>6</sup>Osservatorio Astronomico di Bologna, via Ranzani, 40127 Bologna, Italy

<sup>7</sup>Istituto Te.S.R.E., Via Gobetti, 40129 Bologna, Italy

<sup>8</sup>Istituto di Astrofisica Spaziale, CNR, Roma, Italy

<sup>9</sup>Univ. of Canterbury, Dept. of Physics & Astronomy, Private Bag 4800, Christchurch, New Zealand

<sup>10</sup>Faculty of Science, University of Auckland, New Zealand

<sup>11</sup>Univ. of Durham, Dept. of Physics, South Road, Durham, EEngland DH1 3LE

<sup>12</sup>LAEFF-INTA, P.O. Box 50727, 28080 Madrid, Spain

<sup>13</sup>Instituto de Astrofísica de Andalucía (IAA-CSIC), P.O. Box 03004, 18080 Granada, Spain

<sup>14</sup>Department of Astronomy, P. Universidad Católica, Casilla 306, Santiago 22, Chile

<sup>15</sup>Kapteyn Astronomical Institute, Postbus 800, 9700 AV Groningen, The Netherlands

<sup>16</sup>Palomar Observatory 105-24, Caltech, Pasadena, CA 91125, USA

<sup>17</sup>Anglo-Australian Observatory, PO Box 296, Epping, NSW 2121, Australia

<sup>18</sup>Univ. of Tasmania, Physics Dept., G.P.O. 252C, Hobart, Tasmania 7001, Australia

<sup>19</sup>Astronomical Observatory, University of Copenhagen, Juliane Maries Vej 30, 2100 Copenhagen, Denmark

<sup>20</sup>Universities Space Research Association, NASA Marshall Space Flight Center, SD50, Huntsville, AL 35812, USA

<sup>21</sup>Perth Observatory, Walnut Road, Bickley, Perth 6076, Australia

<sup>22</sup>Univ. of Southampton, Department of Physics and Astronomy, Highfield, Southampton SO17 1BJ

<sup>23</sup>European Southern Observatory, Karl-Schwarzschild-Straße 2 85748, Garching bei München, Germany

<sup>24</sup>Solar-Terrestrial Environment Laboratory, Nagoya University, Furocho, Chikusa-ku, Nagoya 464-8601, Japan

<sup>25</sup>Yukawa Institute, Kyoto University, Japan

<sup>26</sup>Nagano National College of Technology, Japan

<sup>27</sup>Physics Department, University of Alabama in Huntsville, Huntsville, Alabama 35899, USA

<sup>28</sup>Department of Physics, Victoria University of Wellington, New Zealand

<sup>29</sup>Tokyo Metropolitan College of Aeronautics, Japan

<sup>30</sup>Lincoln University College, Buenos Aires, Argentina

<sup>31</sup>Institute of Physics and Astronomy, University of Århus, 8000 Århus C, Denmark

<sup>32</sup>Department of Physics and Space Research Institute, Technion, Haifa 32000, Israel

## ABSTRACT

We present the discovery observations of the optical counterpart of the  $\gamma$ -ray burster GRB990712 taken 4.16 hours after the outburst and discuss its light curve observed in the V, R and I bands during the first  $\sim 35$  days after the outburst. The observed light curves were fitted with a power-law decay for the optical transient (OT), plus an additional component which was treated in two different ways. First, the additional component was assumed to be an underlying galaxy of constant brightness. The resulting slope of the decay is  $0.97 \pm 0.05$  and the magnitudes of the underlying galaxy are:  $V = 22.3 \pm 0.05$ ,  $R = 21.75 \pm 0.05$  and  $I = 21.35 \pm 0.05$ . Second, the additional component was assumed to be a galaxy plus an underlying supernova with a time-variable brightness identical to that of GRB980425, appropriately scaled to the redshift of GRB990712. The resulting slope of the decay is similar, but the goodness-of-fit is worse which would imply that either this GRB is not associated with an underlying supernova or the underlying supernova is much fainter than the supernova associated with GRB980425. The galaxy in this case is fainter:  $V = 22.7 \pm 0.05$ ,  $R = 22.25 \pm 0.05$  and  $I = 22.15 \pm 0.05$ ; and the OT plus the underlying supernova at a given time is brighter. Measurements of the brightnesses of the OT and the galaxy by late-time HST observation and ground-based observations can thus assess the presence of an underlying supernova.

*Subject headings:*  $\gamma$ -rays: bursts — cosmology: observations

## 1. INTRODUCTION

The past two years have witnessed tremendous progress in our understanding of Gamma-Ray Burst (GRB) phenomena. Thanks to the ability of Beppo-Sax to provide arcminute sized error boxes for the bursts, the first optical counterpart was detected in February 1997 for GRB970228 (van Paradijs et al. 1997; Costa et al. 1997). The HST observations of this GRB provided the first clear indication that the GRB is associated with an external galaxy and is unrelated to its nuclear activity (Sahu et al. 1997a). Shortly thereafter, the redshift measurement for GRB 970508 proved beyond doubt that GRBs are extragalactic in nature (Metzger et al. 1997; Djorgovski et al. 1997). More than a dozen GRB optical counterparts have been detected since then, with redshifts as high as 3.42 in the case of GRB971214 (Kulkarni et al. 1998).

The extensive observations of GRB afterglows in X-ray, optical and radio wavelengths have been shown to be consistent with cosmological fire-ball models (e.g. Paczyński & Rhoads 1993; Mészáros & Rees 1997; Wijers et al. 1997). However, the exact cause of the GRBs has remained elusive, and progress in determining the actual mechanism causing the bursts has been slow. The two leading models for GRBs involve the collapse of a massive star (e.g. Woosley 1997; Paczyński 1998), and the merging of a neutron star with either another neutron star or a black hole (e.g. Eichler et al. 1989; Narayan, Paczyński, & Piran 1992; Sahu et al. 1997b). The “isotropic equivalent energy” of some GRBs is as high as  $10^{54}$  ergs, which exceeds the energy equivalent of the total mass involved in the latter model, and hence is thought to favor the former. However, the beaming factor of the emission of the GRB in different wavebands can be high (in both models), so the energetics alone may not be conclusive in favoring one of the models over the other. Since the lifetime of a very massive star is of the order of a million years or shorter, the GRBs are expected to be within or close to star-forming regions in the massive-star collapse model. On the other hand, since the kick-velocity of a newly formed neutron star is of the order of  $200 \text{ km s}^{-1}$ , and since the neutron star, on average, is already about  $10^8$  years old at the time of the burst, GRBs are generally expected to be far from star-forming regions in the merging neutron-star model (Bloom, Sigurdsson & Pols 1999). Thus the location of the GRB with respect to the star-forming regions in the host galaxy could be a distinguishing feature which can help in settling the question of the cause of the GRBs. However, if the

presence of dense interstellar material is prerequisite for the onset of the optical afterglow, then OTs would be observed *only* in star-forming regions regardless of whether GRBs result from neutron-star mergers or from the collapse of massive stars. In any case, if some OTs are found far away from star-forming regions, neutron-star merger model would be favored. If all OTs are found in star-forming regions, the situation is less clear, and depending on the model, one may need to investigate other aspects to find distinguishing features. For example, one consequence of the massive-star collapse model is that the GRB should be accompanied by an underlying supernova, whose brightness variation is distinct from the power-law decay behavior of the OT and may be detectable.

There is a clear bimodality in the observed burst durations: long bursts have timescales of about 10 to 200 seconds, and short bursts have timescales of 0.1 to 1 second (Kouveliotou et al. 1995). All the afterglows that have been discovered so far belong to the subgroup with long bursts (Fishman 1999). All the OTs for which the host galaxies have been observed – although this sample is small – are found to be in galaxies whose spectral indicators suggest star-forming activity (e.g. Fruchter et al. 1999). So there is an interesting possibility that the long-duration GRBs are caused by the collapse of rapidly-rotating massive stars, and hence they occur in star-forming regions. The short-duration bursts may be of a different origin, and may be caused by the coalescence of two neutron stars. The detection of optical counterparts of short duration bursts, and their observations would be important to understand this scenario better.

GRB990712, being at  $z = 0.434$  (Galama et al. 1999a; Hjorth et al. 2000), is one of the closest GRBs observed so far and hence provides a good opportunity to determine the possible presence of an underlying supernova, the location of the GRB within the galaxy, and the luminosity of the galaxy in different wavebands. In this paper we present the optical observations of GRB990712 leading to the discovery of its optical counterpart, and subsequent optical imaging observations taken in different filters during the first  $\sim 35$  days after the burst.

## 2. OBSERVATIONS

GRB990712 was simultaneously detected on 1999 July 12.69655 with the Gamma-Ray Burst Monitor and the WFC unit 2 onboard the BeppoSAX satellite. The burst lasted for about 30 seconds in both the  $\gamma$ -ray (40 - 700 keV) and X-ray (2-26 keV) energy ranges and had a double-peaked struc-

ture. While its intensity in  $\gamma$ -rays is moderate, it exhibited the strongest X-ray prompt emission observed to date (Heise et al. 1999).

The initial Beppo-SAX position, with an error circle of 5 arcmin radius, was revised to one with an error radius of only 2 arcmin. Our first observations were made at this latter position with the SAAO 1m telescope at Sutherland, South Africa on July 12.87 UT, about 4.16 hours after the burst during time generally dedicated to PLANET microlensing observations (Albrow et al. 1998). The optical image was taken through an R filter, with an integration time of 900 sec. The detector was a  $1024 \times 1024$  SITe CCD with an image scale of 0.309 arcsec per pixel and a total field of view of  $5.3 \times 5.3$  square arcmin. Comparison of the image with the Digitized Sky Survey (DSS) image for the same field showed the presence of a new source well above the sky background, that was absent in the DSS image. This new source had a brightness of  $R = 19.4 \pm 0.1$  mag, which is about 2 magnitudes brighter than the limiting magnitude of the DSS image, indicating that the new source was the optical counterpart of the GRB (Bakos et al. 1999a,b). Fig. 1 shows the discovery image, along with the DSS image taken of the same region. Also marked in the figure are the reference stars used for photometric calibration of the OT. A spectrum of this source obtained a few hours later revealed emission and absorption lines which were used to derive redshift of 0.434 for this source (Galama et al. 1999a). Subsequent observations by various groups showed the decaying nature of this source further confirming the identification of the OT with the GRB.

We continued the observations with a multi-wavelength optical follow-up campaign using the telescopes at SAAO, ESO and AAO. A log of all the observations used in this analysis along with the derived magnitudes of the OT are listed in Table 1. The measurements include the acquisition images taken for the spectroscopic observations with the ESO VLT shortly after the discovery of the OT (Vreeswijk et al. 1999, in prep.).

### 2.1. Astrometry and Photometry of the Optical Counterpart

An astrometric solution of the field was carried out using 10 reference stars in the image which are marked in Fig. 1. Their coordinates, as taken from the USNO 2.0 catalog which uses the Hipparcos frame of reference, are listed in Table 2. The pixel centroids of the reference stars were determined using two-dimensional Gaussian fits. These centroids were combined with the USNO coordinates to determine an astrometric solution of the field. The resulting position of the optical counterpart is  $\text{RA}(2000) = 22^h 31^m 53.^s061 \pm 0.^s011$ ,  $\text{Dec}(2000) = -73^d 24' 28.^{''}58 \pm 0.^{''}05$ .

Since sky conditions deteriorated due to clouds just after the discovery observations of the OT, no standard star observations could be taken on that night. The images were calibrated through observations of the standard stars F203 and F209 (Menzies et al. 1989) taken on 13th July at SAAO. All the photometric measurements were carried out using the IRAF aperture photometry task PHOT. The photometry of a few secondary standards in the field (Fig. 1) was carried out using the standard star observations, and the photometry of all GRB observations was then performed via these secondary standards. Since only two standard stars were observed, the extinction correction due to differential airmass between the GRB and the standard star observations were not applied in the preliminary analysis (Bakos et al. 1999a,b). Instead, the photometric measurements taken with the adjacent 50cm telescope were used to get the extinction coefficients, which resulted in a correction of

$-0.075$  mag in V,  $-0.06$  mag in R, and  $-0.02$  mag in I. (This is consistent with the discrepancy pointed out by Kemp & Halpern 1999). Our final magnitudes of the secondary photometric standards are listed in Table 2, and Table 1 lists the derived magnitudes of the OT in different bands at different epochs including one extra measurement reported by Kemp and Halpern (1999).

## 3. ANALYSIS

### 3.1. The Light Curve in Different Wavebands

All the photometric measurements listed in Table 1 are also shown in Fig. 2. The observed light curves in different bands clearly show a continuously-changing slope suggesting an additional component to the power-law decay of the OT as first noted by Hjorth et al. (1999a). In an approach similar to the one followed by Hjorth et al. (1999b), we have fitted this additional component in two ways: (i) with an underlying galaxy of constant brightness, and (ii) an underlying galaxy plus a supernova similar to GRB980425, appropriately scaled to the redshift of GRB990712.

First, a power law decline of the form  $f(t) \propto t^{-\alpha}$  for the OT and a constant contribution from the background galaxy was used to fit the observed light curves simultaneously in different bands, with the same slope for all the bands. The resultant slope is 0.97, and the total  $\chi^2$  is 47 for 39 d.o.f. (Relaxing the condition of the same slope in different bands does not alter the fit parameters significantly). The total  $\chi^2$  is, however, fairly flat (between 44 and 52) for any value of  $\alpha$  between 0.95 and 1.02 beyond which the total  $\chi^2$  increases rapidly. Fig. 2 shows the best fit to the light curves. The derived magnitude of the underlying galaxy is not very sensitive to the exact value of  $\alpha$  and are found to be  $V = 22.3 \pm 0.05$ ,  $R = 21.75 \pm 0.05$  and  $I = 21.35 \pm 0.05$  where the uncertainties represent the variation of the derived magnitudes as a result of changing  $\alpha$  between 0.95 and 1.02.

One possible consequence of the massive-star model for the GRB is that one should observe an underlying supernova in the lightcurve of an OT. The physical connection of a GRB with a supernova (SN), first suggested by the discovery of a peculiar type Ic SN in the error box of GRB 980425 (Galama et al. 1998; Iwamoto et al. 1998), has been strengthened further by recent observations of other GRBs. Castro-Tirado and Gorosabel (1999) suggested that the light curve of GRB980326 resembled that of a SN, and indeed Bloom et al. (1999) showed that the late time light curve of GRB 980326 can be explained by an underlying SN1998bw type SN at a redshift of around unity. For the afterglow of GRB 970228, Reichart (1999) and Galama et al. (1999b) find that a power-law decay plus SN1998bw light curve redshifted to the distance of the burst,  $z = 0.695$  (Djorgovski et al. 1999), fits the observed light curve very well. In light of these new findings, we have also fitted the observed light curve of GRB 990712 assuming the presence of an underlying supernova.

In order to determine the contribution of the underlying supernova, we first calculate the expected V, R, I magnitudes of SN1998bw, placing it at the redshift of GRB 990712,  $z = 0.434$ . This includes wavelength shifting and time profile stretching (both by a factor of  $1+z$ ), and rescaling the magnitudes for a distance corresponding to  $z = 0.434$ , assuming  $\Omega_0 = 0.2$ . To account for the wavelength shift correctly, we interpolate the redshifted UBVRI broadband flux spectrum of the SN for each bin in time with a spline fit, obtain the V, R, and I fluxes at their effective wavelengths, and convert these

back to obtain magnitudes in the observer's frame (Fukugita et al. 1995). The resultant SN light curves in different bands are shown at the bottom of Fig. 3. In order to fit the GRB light curve, the SN flux is subtracted from the observed GRB flux, and the residual fluxes are assumed to be due to the OT and the underlying galaxy. The procedure outlined earlier is then used to fit the light curves. The  $\chi^2$  in this case is 52 for 42 d.o.f., which is clearly higher than the model without the supernova. The resulting slope of the decay is 0.96 which is quite similar but the magnitudes of the underlying galaxy are fainter:  $V = 22.7 \pm 0.05$ ,  $R = 22.25 \pm 0.05$  and  $I = 22.15 \pm 0.05$ . The brightness of the OT of the GRB at a given time is also slightly lower, but the combined brightness of the OT and the underlying supernova (which is the quantity that can be measured if the OT can be resolved from the galaxy) is higher than the brightness of the OT in the absence of an underlying supernova.

It is important to note, however, that there is no evidence that the SNe possibly underlying the GRB afterglows have the same brightness or the same decay behavior. Our assumption that the underlying supernova is identical to SN1998bw is dictated by two reasons. First, this is the only SN associated with a GRB whose light curve has been monitored extensively. Second, the number of data points in our light curves does not allow us to vary the characteristics of the underlying SN light curve. So the fact that the  $\chi^2$  is higher in this case can be misleading since the true underlying supernova may be different from that of SN1998bw, making the resultant  $\chi^2$  higher for our simplified model. This chi-square analysis indicates that either GRB990712 is not associated with an underlying supernova or the underlying supernova is much fainter than the supernova associated with GRB980425. However, the qualitative conclusion that the galaxy is expected to be fainter and the OT plus the SN is expected to be brighter in the presence of an underlying supernova is unlikely to change. Hence late time HST observations, in which the OT is well resolved so that the brightness of the OT and the galaxy can be estimated separately, or late time ground-based observations when the brightness of the OT is negligible, would greatly help in determining the presence of an underlying supernova.

In both the above scenarios (i.e. with and without an underlying supernova), the power-law index of the decay  $\alpha$  is about 1, making it one of the slowest decline rates of all the OTs observed so far. Since  $\alpha \leq 1$  would lead to a divergence of the total energy integrated over time, the slope must steepen at later times. This has been observed for GRB990510 which declined with  $\alpha = 0.82$  at early times, later steepening with time (Harrison et al. 1999). Power-law decays are thought to arise from electrons shocked by the relativistic expansion of the debris into the ambient medium. In such a case, the information on the change of slope can be used to derive information on the cooling rate of the electrons in the post-shock region (see, e.g. Wijers et al. 1997; Sari, Piran, & Narayan 1998; Livio & Waxman 1999).

### 3.2. Spectral Energy Distribution of the OT

If the OT emission is due to the synchrotron radiation from the swept-up electrons in the post-shock region, then its energy distribution is expected to be of the general form  $f_\nu \propto t^{-\alpha} \nu^\beta$ . In such a case, one expects a relationship between the power law index of the energy distribution of the electrons  $p$ , the spectral slope  $\beta$ , and the decay constant  $\alpha$  (Sari et al. 1998). One must distinguish two cases: (i) both the peak frequency  $\nu_m$  and the cooling frequency  $\nu_c$  are below the optical/IR wave-

band, in which case  $p = (4\alpha + 2)/3 = 1.97 \pm 0.04$  and  $\beta = -p/2 = -0.99 \pm 0.02$ , and (ii)  $\nu_m$  has passed the optical/IR waveband, but  $\nu_c$  has not yet done so, in which case  $p = (4\alpha + 3)/3 = 2.31 \pm 0.04$  and  $\beta = -(p-1)/2 = -0.66 \pm 0.02$ .

We can now compare the theoretically expected spectral slope ( $\beta$ ) with the observed one. Although perhaps best determined by the spectroscopic measurements, our light curve analysis provides magnitudes of the OT in different bands, which can be directly used to derive  $\beta$ . We should note here that the brightness of the underlying galaxy and the possible contamination by an underlying supernova makes the determination of the magnitudes of the OT less reliable at later times, and our value of  $\alpha$  is most likely dominated by the early part of the light curve when the OT was bright. Furthermore,  $\alpha$  was kept fixed in *all* the bands for the entire period of our observations, which implies that we cannot detect any spectral *evolution* of the OT. The *synphot/calcphot* task in IRAF was used to determine the  $V-R$  and  $R-I$  values for a range of  $\beta$  values, which were then compared with the colors derived from the light curve analysis to determine the spectral slopes. The  $V-R$  color implies a spectral slope of  $-1.8 \pm 0.5$ , and the  $R-I$  color implies a spectral slope of  $-0.7 \pm 0.1$ . Thus the slope derived from the  $V$  and  $R$  bands is closer to the case (i) mentioned above, and the slope derived from the  $R$  and  $I$  bands is closer to the case (ii). This is roughly consistent with the theoretical expectations and implies that, in the early part of the light curve,  $\nu_m$  has passed the  $V$  and  $R$  and  $I$  bands, but  $\nu_c$  has not passed the  $I$  band.

### 3.3. The Background Galaxy

The inferred magnitudes for an underlying galaxy suggest that the galaxy is relatively bright compared to the OT, and it may be possible to see the host galaxy directly in the images. The NTT images taken about 8 days after the burst had the best seeing ( $\sim 1$  arcsec) and the  $R$  images indeed show some hint of a slight extension. To further investigate this, all the images taken in  $B, V, R$  and  $I$  bands were co-added, giving rise to a single deep image of a total integration time of 40 min. From this combined image, we constructed a model point-spread-function (PSF) from a few isolated bright stars in the field using IRAF/DAOPHOT. This model PSF was used to subtract the point source contribution from the OT. The PSF-subtracted image shows some residual distribution elongated in the east-ward direction of the OT over a total of about 2 arcsec, which is probably the contribution of the underlying galaxy. Thus HST observations would show the detailed structure of the galaxy (Fruchter et al. in prep).

The derived magnitudes of the underlying galaxy were used to calculate its luminosity. The GRB is at a Galactic latitude and longitude of  $-40$  and  $315$  degrees, respectively. The extinction models of Burstein & Heiles (1982) and Schlegel et al. (1998) yield  $E(B-V)$  of  $0.015$  and  $0.033$ , respectively, for the position of the GRB. This extinction is small and similar to SN1998bw, which is neglected in our analysis. To derive the luminosity of the host galaxy, we use a redshift of  $z=0.434$  which, for  $H_0 = 70 \text{ km s}^{-1}$  and  $\Omega=0.2$ , corresponds to a luminosity distance of 2160 Mpc, and a distance modulus of 41.67 mag. Applying the K-correction for  $z=0.434$ , the inferred luminosity of the galaxy is of the order of  $L_*$  (depending on the presence of an underlying supernova), where  $L_*$  corresponds to the luminosity of a typical galaxy at the 'knee' of the observed galaxy luminosity function (see, e.g., Lilly et al. 1999). If we exclude SN1998bw (which is not only 'nearby' ( $z = 0.008$ ), but for which the energy released in  $\gamma$ -rays is much smaller than any other GRB),

then GRB990712 is the closest ‘cosmological’ GRB, and the apparent magnitude of its host galaxy is the brightest among all the GRB host galaxies observed so far. Compared to the host galaxy of GRB990713, which is the next brightest, the host galaxy of GRB990712 is about 0.25 magnitudes brighter in R if there is an underlying supernova, and more than a magnitude brighter if there is no underlying supernova.

We dedicate this paper to the memory of our colleague and friend Jan van Paradijs who passed away due to an illness on

November 2, 1999, during the final stages of the preparation of this manuscript. Jan received several awards for his fundamental contributions in this field, including the 1998 Rossi prize of the American Astronomical Society. We will sorely miss his contagious enthusiasm, his brilliant insights, and his benevolent personality.

This project is partly supported by the Chilean Fondecyt Project No. 3990024 and the Danish Natural Science Research Council (SNF). M. Dominik is supported by a Marie Curie Fellowship (ERBFMBICT972457).

#### REFERENCES

Akerlof, C., et al. 1999, *Nature*, 398, 400  
 Bakos, G., et al. 1999a, *GCN* 387  
 Bakos, G., et al. 1999b, *IAUC* 7255  
 Bloom, J. S., et al. 1999, *Nature*, 401, 453  
 Bloom, J. S., Sigurdsson, S., & Pols, O. R. 1999, *MNRAS*, 305, 763  
 Burstein, D., & Heiles, C. 1982, *AJ*, 87, 1165  
 Castro-Tirado, A. J., & Gorosabel, J. 1999, *A&AS*, 138, 449  
 Costa, E., et al. 1998, *Nature*, 387, 783  
 Djorgovski, S. G., et al. 1997, *Nature*, 387, 876  
 Eichler, D., Livio, M., Piran, T., & Schramm, D. N. 1989, *Nature*, 340, 126  
 Fishman, G. J. 1999, in *Proc. STScI Symp. on ‘Supernovae and Gamma-Ray Bursts’*, ed. M. Livio, K. C. Sahu & N. Panagia (in press)  
 Frail, D. A., Kulkarni, S. R., & Bloom, J. S. 1999, *ApJ*, 525, L81  
 Fruchter, A., et al. 1999, *ApJ*, 519, L13  
 Fukugita, M., Shimasaku, K., & Ichikawa, R. 1995, *PASP*, 107, 945  
 Galama, T. J., et al. 1997, *Nature*, 387, 479  
 Galama, T. J., et al. 1998, *Nature*, 395, 670  
 Galama, T. J., et al. 1999a, *GCN* 388  
 Galama, T. J., et al. 1999b, *ApJ*, submitted (astro-ph/9907264)  
 Harrison, F. A., et al. 1999, *ApJ*, 523, 121  
 Heisse, J., et al. 1999, *IAUC* 7221  
 Hjorth, J., et al. 1999a, *GCN* 389  
 Hjorth, J., et al. 1999b, *GCN* 403  
 Hjorth, J., et al. 2000, to appear in *ApJ* (astro-ph/0003383)  
 Iwamoto, K., et al. 1998, *Nature*, 395, 672  
 Kemp, J., & Halpern, J. 1999, *GCN* 402  
 Kouveliotou, C., et al. 1995, in *AIP Conf. Proc. 384, Gamma Ray Bursts – 3rd Huntsville Symposium*, ed. C. Kouveliotou, M. F. Briggs, & G. J. Fishman (New York: AIP), 42  
 Kulkarni, S. R., et al. 1998, *Nature*, 393, 35  
 Lilly, S. J., et al. 1999, *ApJ*, 518, 641  
 Livio, M., & Waxman, E. 1999, *ApJ*, submitted (astro-ph/9911160)  
 Menzies, J. W., Cousins, A. W. J., Banfield, R. M., & Laing, J. D. 1989, *SAAO Circular* 13, 1  
 Mészáros, P., & Rees, M. J. 1997, *ApJ*, 476, 232  
 Metzger, M. R., et al. 1997, *Nature*, 387, 879  
 Narayan, R., Paczyński, B., & Piran, T. 1992, *ApJ*, 395, L83  
 Paczyński, B. 1998, *ApJ*, 494, L45  
 Paczyński, B., & Rhoads, J. E. 1993, *ApJ*, 418, L5  
 Reichart, D. E. 1999, *ApJ*, 521, L111  
 van Paradijs, J., et al. 1997, *Nature*, 386, 686  
 Sahu, K. C., et al. 1997a, *Nature*, 387, 476  
 Sahu, K. C., et al. 1997b, *ApJ*, 489, L127  
 Sari, R., Piran, T., & Narayan, R. 1998, *ApJ*, 497, L17  
 Schlegel, D., Finkbeiner, D., & Davis, M., 1998, *ApJ*, 500, 525  
 Waxman, E. 1997, *ApJ*, 485, L5  
 Wijers, R. A. M. J., Rees, M. J., & Mészáros, P. 1997, *MNRAS*, 288, L51  
 Woosley, S. E., & Wallace, R. K. 1982, *ApJ*, 258, 716

FIG. 1.— The top panel shows the discovery image of the optical counterpart (OT) of GRB990712, obtained with SAAO 1m telescope about 4.16 hours after the burst. The bottom panel shows the Digitized Sky Survey (DSS)  $3 \times 2.8$  square arcmin image of the same field. The SAAO image shows the optical counterpart (marked ‘GRB’) as a new source which is about 2 magnitudes brighter than the limiting magnitude of the DSS image. The reference stars marked 1 and 2 were used as secondary photometric standards and the reference stars 1 to 10 were used for the astrometry. North is up and east is to the left.

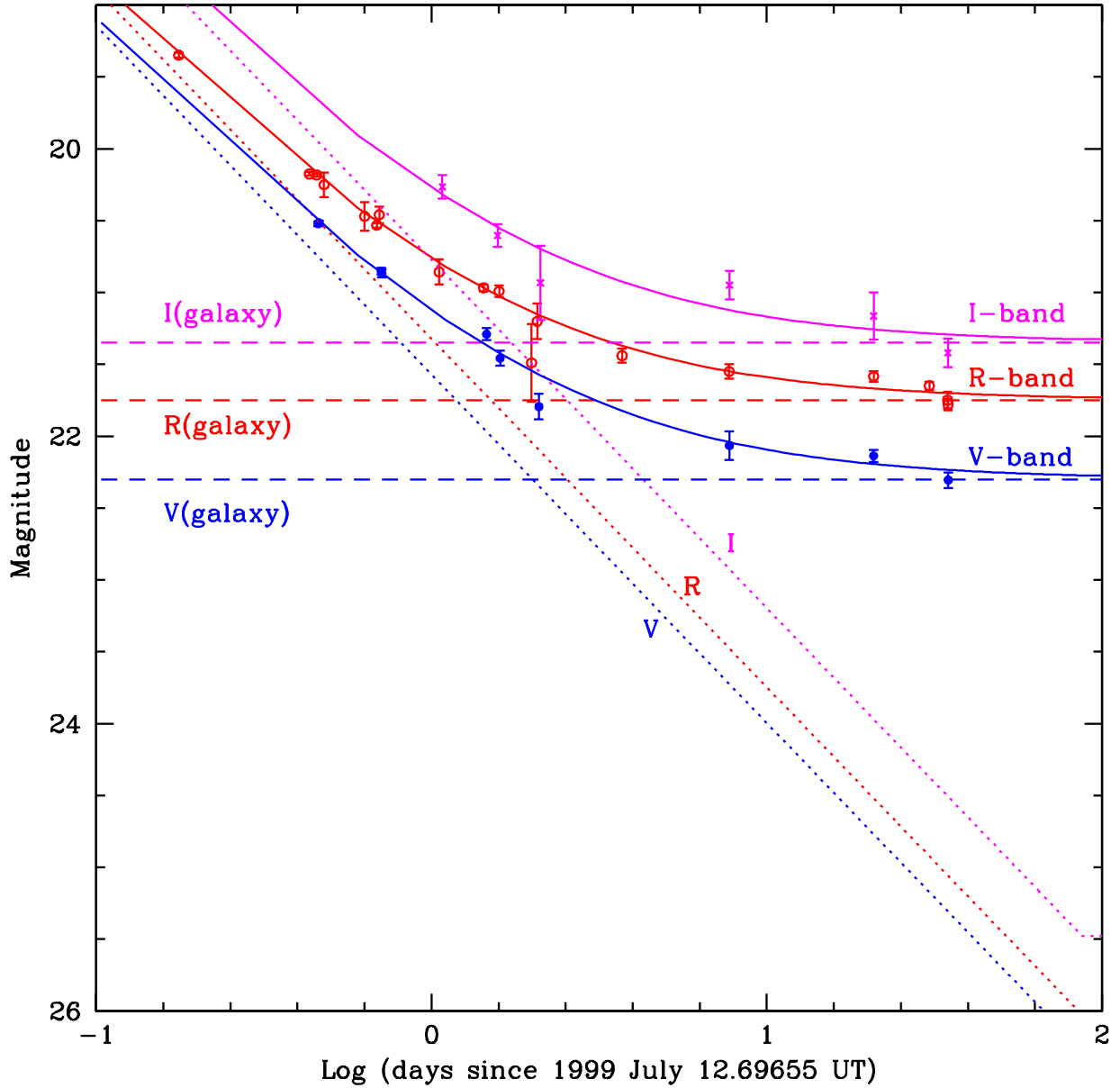


FIG. 2.— The observed light curves of GRB990712 in different optical bands and the model fits assuming a power-law decay for the OT and the presence of an underlying galaxy. The I-band measurements are shown as asterisks, the R-band measurements as open circles, and the V-band measurements as filled circles. The magnitudes of the underlying galaxy in different bands are shown as horizontal dashed lines. The dotted lines show the decay characteristic of the OT and the solid curves show the combined OT+galaxy. The derived slope of the power-law decay is  $0.97 \pm 0.05$  and the magnitudes of the underlying galaxy are  $V = 22.3 \pm 0.05$ ,  $R = 21.75 \pm 0.05$  and  $I = 21.35 \pm 0.05$ .

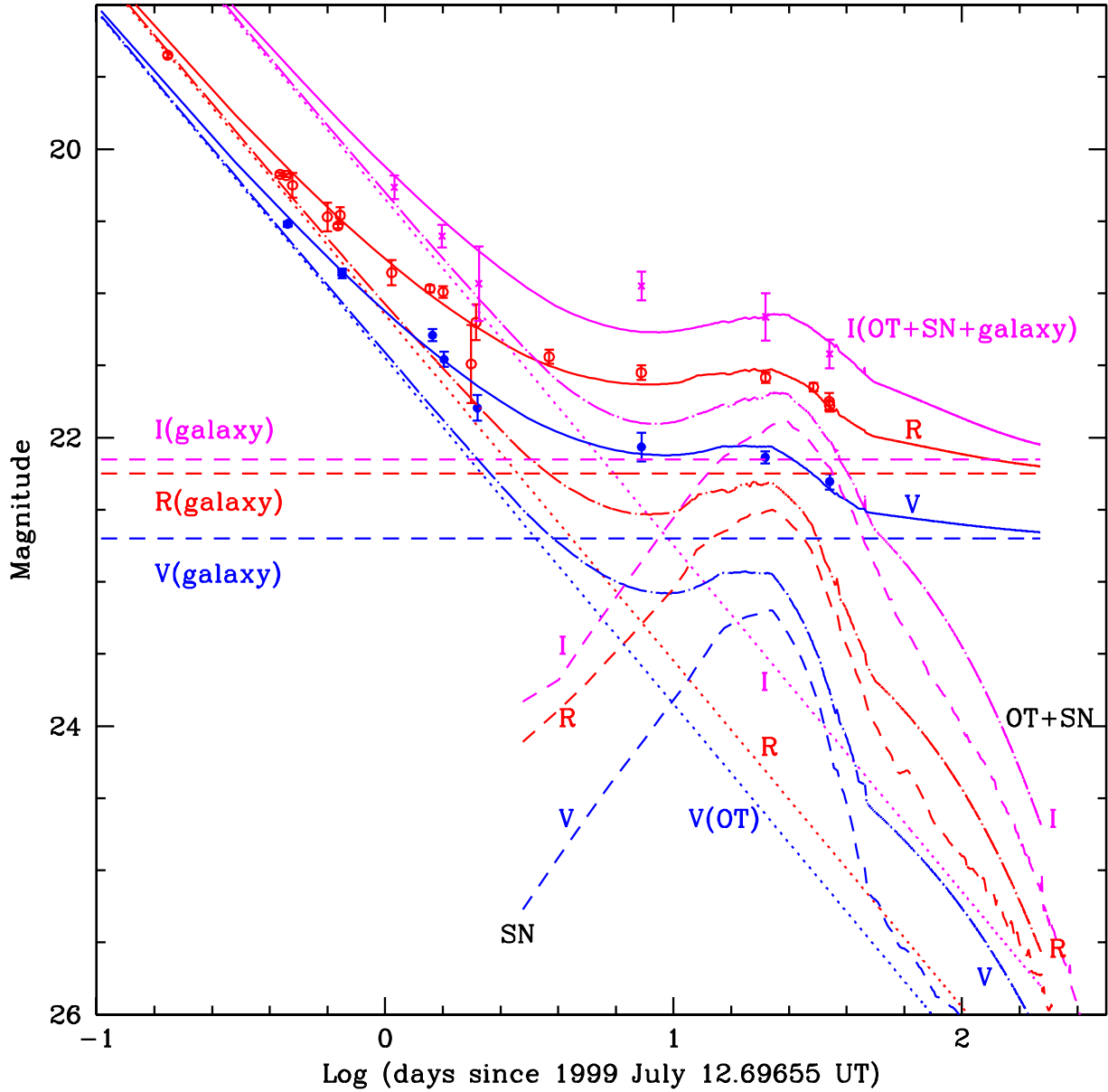


FIG. 3.— The observed light curves of GRB990712 in different optical bands and the fits to the light curves assuming a power-law decay for the OT, an underlying galaxy, and an underlying supernova whose brightness is assumed to be identical to GRB980425 scaled appropriately to the redshift of GRB990712. The symbols used are the same as in Fig. 2. In addition, the light curves of the supernova (scaled as explained before) in different bands are shown as dashed lines, the light curves of the SN+OT are shown as dot-dashed curves, and the light curves of the OT+SN+galaxy are shown as solid curves. The derived slope of the power-law decay is  $0.96 \pm 0.05$  and the magnitudes of the underlying galaxy are  $V = 22.7 \pm 0.05$ ,  $R = 22.25 \pm 0.05$  and  $I = 22.15 \pm 0.05$ .

TABLE 1  
JOURNAL OF THE OBSERVATIONS

Day (UT)	Mag.	Telescope
R-band measurements:		
Jul 12.873	19.349 $\pm$ 0.019	SAAO 1m
Jul 13.129	20.175 $\pm$ 0.011	VLT 8m
Jul 13.151	20.183 $\pm$ 0.009	VLT 8m
Jul 13.174	20.251 $\pm$ 0.085	ESO 1.5m
Jul 13.328	20.470 $\pm$ 0.10	MJUO 61cm
Jul 13.383	20.533 $\pm$ 0.016	VLT 8m
Jul 13.395	20.460 $\pm$ 0.057	CASLEO 2.15m
Jul 13.750	20.857 $\pm$ 0.088	SAAO 1m
Jul 14.127	20.968 $\pm$ 0.025	VLT 8m
Jul 14.287	20.991 $\pm$ 0.040	NTT 3.5m
Jul 14.683	21.490 $\pm$ 0.27	MJUO 61cm
Jul 14.764	21.201 $\pm$ 0.123	SAAO 1m
Jul 16.403	21.420 $\pm$ 0.050	NTT 3.5m
Jul 20.421	21.550 $\pm$ 0.050	NTT 3.5m
Aug 02.533	21.584 $\pm$ 0.036	AAT 3.9m
Aug 12.232	21.650 $\pm$ 0.030	VLT 8m
Aug 16.320	21.750 $\pm$ 0.060	CTIO 0.9m <sup>†</sup>
Aug 16.445	21.779 $\pm$ 0.041	AAT 3.9m
V-band measurements:		
Jul 13.156	20.523 $\pm$ 0.017	SAAO 1m
Jul 13.158	20.516 $\pm$ 0.015	SAAO 1m
Jul 13.405	20.852 $\pm$ 0.023	VLT 8m
Jul 13.406	20.866 $\pm$ 0.028	VLT 8m
Jul 14.157	21.290 $\pm$ 0.041	VLT 8m
Jul 14.298	21.458 $\pm$ 0.053	VLT 8m
Jul 14.787	21.795 $\pm$ 0.089	SAAO 1m
Jul 20.433	22.065 $\pm$ 0.100	NTT 3.5m
Aug 02.511	22.136 $\pm$ 0.042	AAT 3.9m
Aug 16.471	22.305 $\pm$ 0.054	AAT 3.9m
I-band measurements:		
Jul 13.774	20.266 $\pm$ 0.082	SAAO 1m
Jul 14.271	20.603 $\pm$ 0.078	NTT 3.5m
Jul 14.810	20.933 $\pm$ 0.258	SAAO 1m
Jul 20.439	20.950 $\pm$ 0.100	NTT 3.5m
Aug 02.554	21.164 $\pm$ 0.165	AAT 3.9m
Aug 16.414	21.420 $\pm$ 0.100	AAT 3.9m

<sup>†</sup>Taken from Kemp & Halpern (1999)

TABLE 2

POSITIONS AND MAGNITUDES OF THE OT AND THE REFERENCE STARS, AND THE MAGNITUDES OF THE SECONDARY STANDARDS. THE MAGNITUDES HAVE TYPICAL UNCERTAINTIES OF 0.01 MAGNITUDES.

No.	RA(2000)	Dec(2000)	X	Y	V	R	I
OT	22:31:53.0614	-73:24:28.576	579.40	620.02			
1	22:31:50.8933	-73:24:25.280	609.98	630.95	17.185	16.40	15.64
2	22:31:40.1507	-73:25:09.400	758.34	487.54	16.975	16.65	16.29
3	22:31:49.7413	-73:26:09.250	624.22	294.44	16.455	15.97	15.50
4	22:32:18.6200	-73:24:09.920	224.05	680.45	15.905	15.27	14.65
Additional reference stars used for astrometry:							
5	22:31:49.3380	-73:24:53.130	631.68	537.68			
6	22:32:02.5307	-73:25:27.980	446.48	427.78			
7	22:32:00.6387	-73:23:20.810	474.52	839.78			
8	22:31:37.5760	-73:23:34.160	794.42	796.29			
9	22:32:21.9453	-73:24:27.680	179.47	623.97			
10	22:32:16.1573	-73:24:55.230	259.72	535.90			

This figure "ksahu\_fig1a.jpg" is available in "jpg" format from:

<http://arxiv.org/ps/astro-ph/0003378v1>

This figure "ksahu\_fig1b.jpg" is available in "jpg" format from:

<http://arxiv.org/ps/astro-ph/0003378v1>